한국기계가공학회지, 제20권, 제3호, pp. 16～23(2021.03) ISSN 1598-6721(Print)
Journal of the Korean Society of Manufacturing Process Engineers, Vol. 20, No. 3, pp. 16~23(2021.03) ISSN 2288-0771(Online)

https://doi.org/10.14775/ksmpe.2021.20.03.016

Fracture Characteristic of Double Cantilever Beam Specimen Using Lightweight Material at Sliding Mode

Jae-Won Kim*, Jae-Ung Cho**,#

*Department of Mechanical Engineering, Graduate School, Kongju National UNIV.

**Division of Mechanical and Automotive Engineering, Kongju National UNIV.

미끄러짐 모드에서의 경량 재료를 이용한 이중외팔보 시험편의 파손 특성

김재원*, 조재웅**,#

*공주대학교 일반대학원 기계공학과, **공주대학교 기계자동차공학부

(Received 03 October 2020; received in revised form 11 October 2020; accepted 19 October 2020)

ABSTRACT

The fracture characteristic of the bonded interface under the application of a sliding load to a double cantilevered specimen manufactured using lightweight material was examined. Inhomogeneously bonded materials such as Al6061-T6, CFRP, and CFRP-Al were employed. In the experiment, the specimen was loaded on both directions by applying a shearing load to the bonding interface. The experimentally obtained stress, specific strength and energy release rate values were examined. CFRP exhibited excellent specific strength. The experimental results demonstrated that the inhomogeneous bonded material CFRP-Al exhibited an overall high performance in comparison with the single materials.

Keywords : Double Cantilever Beam(이중외팔보), Al6061-T6(Al6061-T6), Carbon Fiber Reinforced Plastic(탄소섬유강화플라스틱), Structural Adhesive(구조용 접착제)

1. Introduction

The lightweight material used at structure has the specific gravity lower than the ferrous metal. This material has the advantage to withstand the load stronger than the steelused at the structure[1-4]. In addition, the fastening method has been utilized with the structural adhesive, not the bolt or rivet. The structural adhesives used recently for automotive bodies have the strength higher than general adhesives. Therefore, a study on the fracture of bonding interface under the sliding load(Mode II) was carried out with the DCB specimen with the lightweight material[5-8].

Corresponding Author : jucho@kongju.ac.kr
Tel: +82-41-521-9271, Fax:+82-41-555-9123

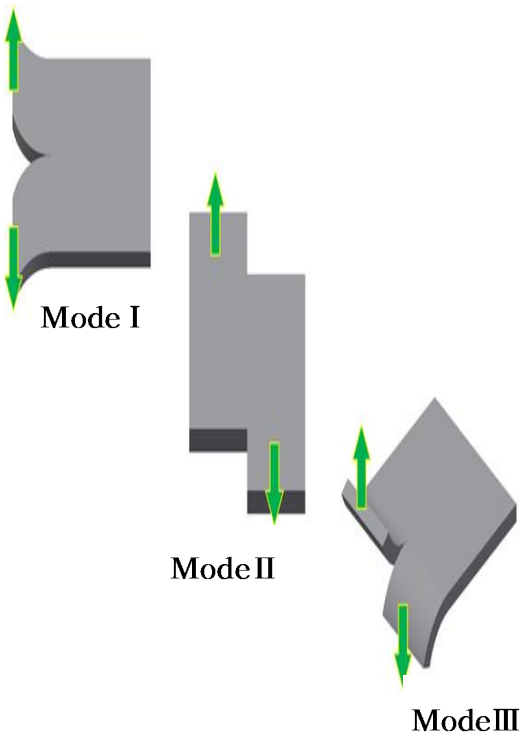

Fig. 1 Schematic diagram by the fracture due to load by mode

2. Theory Relevant to Carbon Fiber Reinforced Plastic (CFRP)

There are the fracture characteristics according to the diverse loads at modes I, II and III. As shown in Fig. 1, three different fracture types are available. The first fracture type is the opening mode (Mode I). At mode I, the fracture method is usually same with a tensile test. If a specimen is placed on the plane X-Y, its top and bottom are pulled in the X and Y directions. At mode II (sliding mode), when a specimen is placed on the plane X-Y, one side is pulled in the '+Y' direction. In a symmetric plane, on the contrary, it is pulled in the '-Y' direction. At mode III (tearing mode), provided that a specimen is placed on the plane X-Z, one end is pulled in the '+Y' direction while the other end is pulled in the '-Y' direction just as paper is being torn off[9-10].

CFRP is the reinforced plastic made of carbon fiber and epoxy. The material of CFRP has an orthotropic property because of the fiber characteristic. In general, the fiber is strong and durable vertically but weak horizontally. Therefore, it reveals an orthotropic property. In a single ply of the carbon fiber, several plies are stacked and laminated. Under this process, CFRP is produced. In particular, the prepreg CFRP was adopted in this study. At utilizing the prepreg method, the carbon fiber with epoxy resin is used for compressing and stacking. In such a CFRP, the curvature and stiffness matrix have a significant influence on the physical property. The formulae (1) and (2) represent the stiffness matrix ([Q]) and curvature (κ) used in calculation of CFRP property: (A: Extensional stiffness matrix, D: Bending stiffness matrix, B: Extensional bending coupling stiffness matrix)[11]

$$\text{Stiffness matrix } [Q] = \begin{vmatrix} \frac{E_{11}}{(1-(\nu_{12}*\nu_{21}))} & \frac{(E_{11}*\nu_{21})}{(1-(\nu_{12}*\nu_{21}))} & 0 \\ \frac{(E_{11}*\nu_{21})}{(1-(\nu_{12}*\nu_{21}))} & \frac{E_{22}}{(1-(\nu_{12}*\nu_{21}))} & 0 \\ 0 & 0 & G_{12} \end{vmatrix} \quad (1)$$

$$\begin{bmatrix} \epsilon^0 \\ \kappa \end{bmatrix} = \begin{bmatrix} A & B \\ B & D \end{bmatrix}^{-1} \begin{bmatrix} N \\ M \end{bmatrix} \quad (2)$$

3. Experiment

3.1 Specimen

Fig. 2 shows the shape and specification of the specimen for mode II while Fig. 3 reveals the adhesion of the specimen for mode II. In the specimen for mode II, its design was corrected in order to illustrate the sliding fracture. The cantilever

length was elongated until 210mm in order to secure the bonded interface which was critical at an adhesive fracture experiment. With this reason, the bonded interface for mode II was designated to 170mm just like modes I and III. Fig. 4 shows the actual shape of the specimen for mode II in order of CFRP, Al6061 and 'CFRP-Al'. The specimen for mode II reveals a slight disparity with the design requirement at the neck area. If a right-angle shape is formed during turning, the specimen can be fractured due to the stress concentration before the adhesive fracture. Therefore, a slight gradient at the neck area was applied to the specimen.

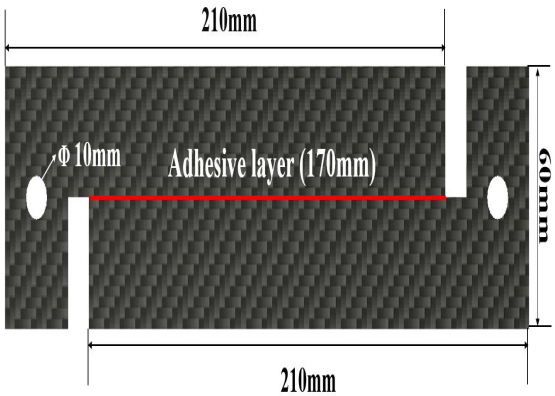

Fig. 2 Shape and specification of the specimen for mode II

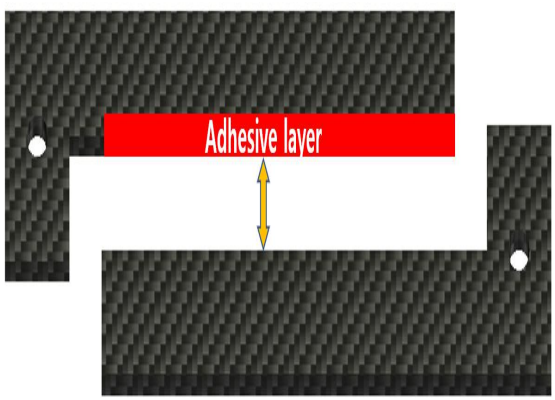

Fig. 3 Adhesion of the specimen for mode II

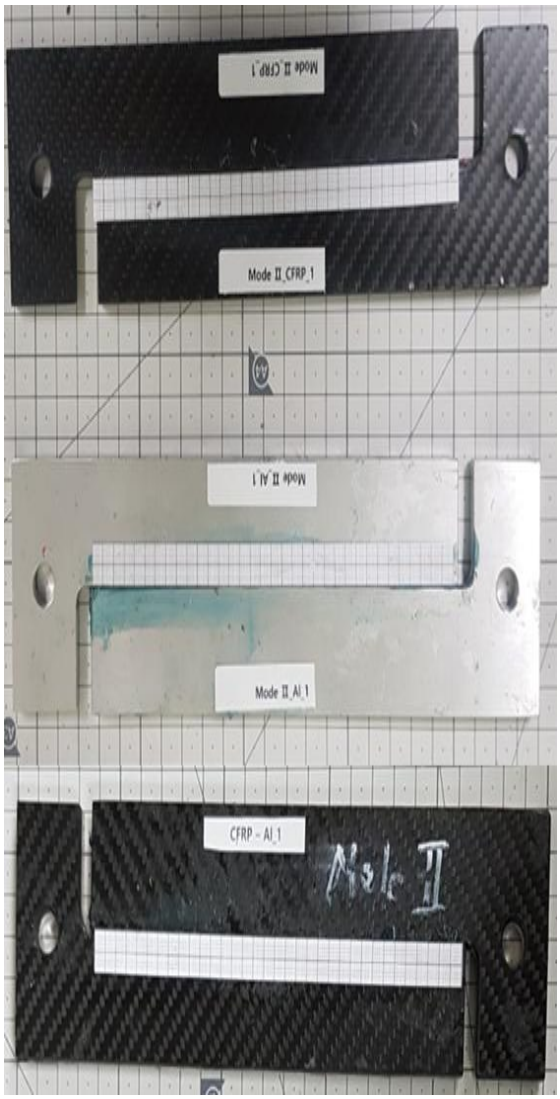

Fig. 4 Actual shape of the specimen for mode II

3.2 Experimental setup and condition

Fig. 5 shows the specimen held for mode II and the experimental condition. When the specimen was held on the plane X-Y, 3mm/min. the forced displacement was applied in the Y-axis direction in the left cantilever while the right cantilever was fixed. So, the sliding fracture was being shown by carrying out the experiment.

Fig. 5 Specimen held for mode II and the experimental condition

4. Experiment Results

4.1 Stress due to displacement

Figs. 6, 7 and 8 show the stress due to displacement for the sliding fracture of mode II by material. In terms of the maximum stress, 'CFRP-Al' was the highest, followed by CFRP and Al. The maximum stresses of 'CFRP-Al', CFRP and Al were 7.2 MPa, 6.2 MPa and 2.8 MPa, respectively. By comparing with the stress results on mode I, unlike the opening fracture, the maximum stresses was higher in the CFRP-bonded specimen at the sliding fracture.

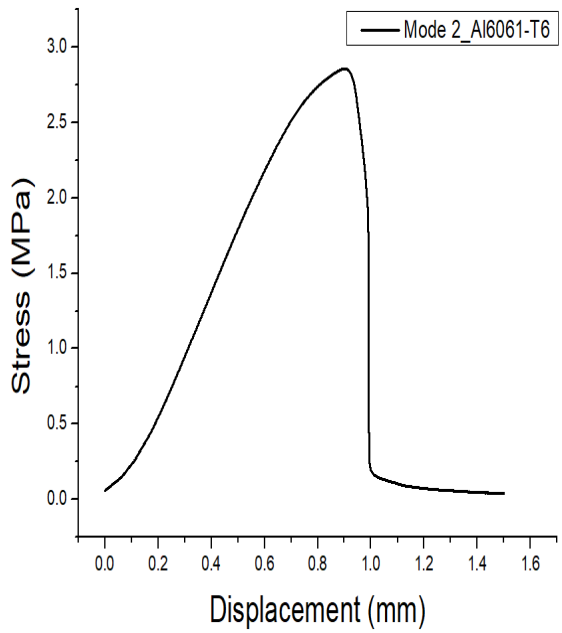

Fig. 6 Stress due to displacement for the sliding fracture of mode II by Al6061-T6

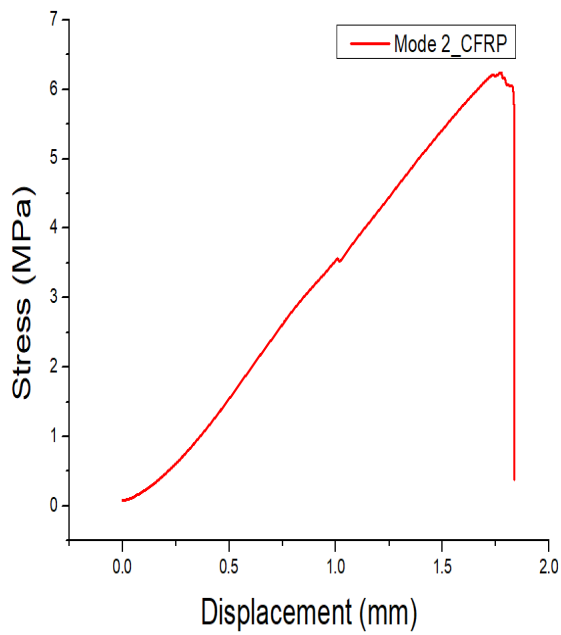

Fig. 7 Stress due to displacement for the sliding fracture of mode II by CFRP

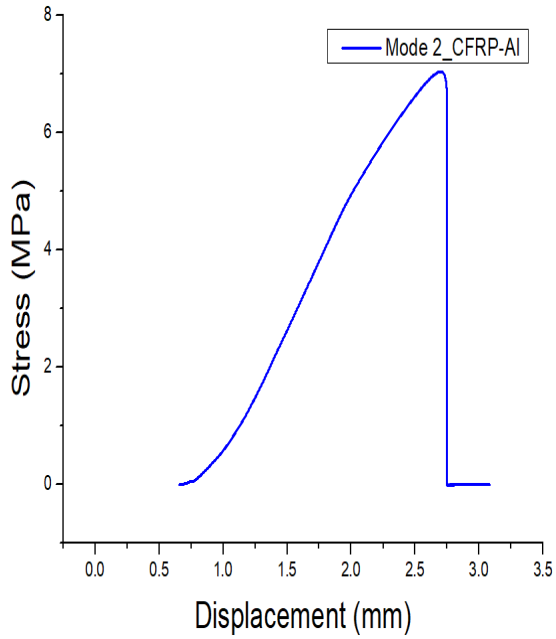

Fig. 8 Stress due to displacement for the sliding fracture of mode II by CFRP-Al

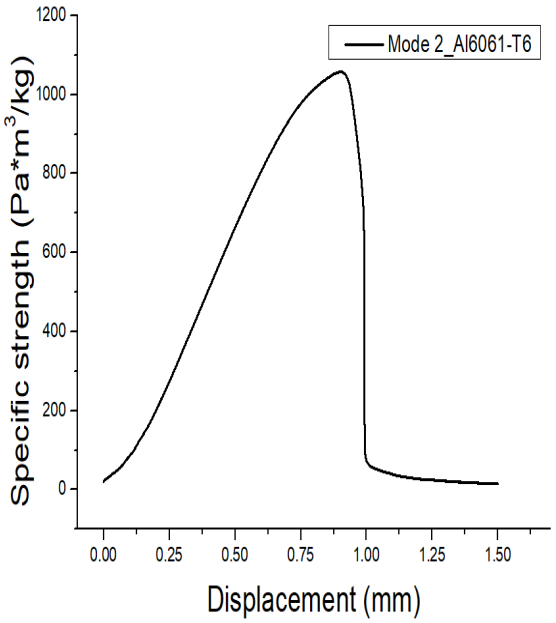

Fig. 9 Specific strength due to displacement for the shearing fracture of mode II by Al6061-T6

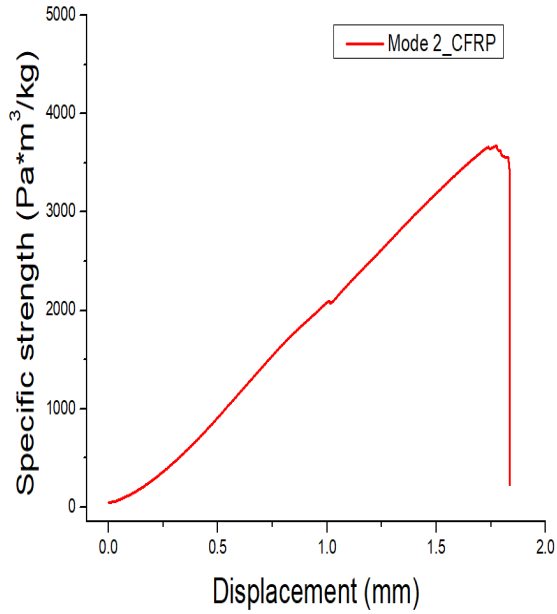

Fig. 10 Specific strength due to displacement for the shearing fracture of mode II by CFRP

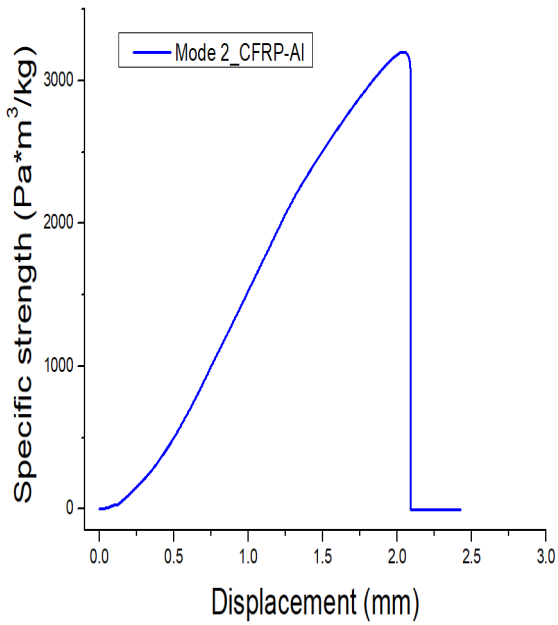

Fig. 11 Specific strength due to displacement for the shearing fracture of mode II by CFRP-Al

4.2 Specific strength due to displacement

Figs. 9, 10 and 11 show the specific strength due to displacement for the shearing fracture of mode II by material. In terms of the specific strength, CFRP was the highest, followed by 'CFRP-Al' and Al. The specific strengths of CFRP, 'CFRP-Al' and Al were 3700 Pa*m^3/kg, 3220 Pa*m^3/kg and 1100 Pa*m^3/kg, respectively. On the basis of these results, it is thought that the bonded material of CFRP as basis is helpful for the structure with lightweight under the in-plane shearing fracture.

4.3 Energy release rate due to crack length

Figs. 12, 13 and 14 show the energy release rate due to crack length for the sliding fracture of mode II by material. In all three materials, the energy release rate was the highest at the very beginning of crack propagation.

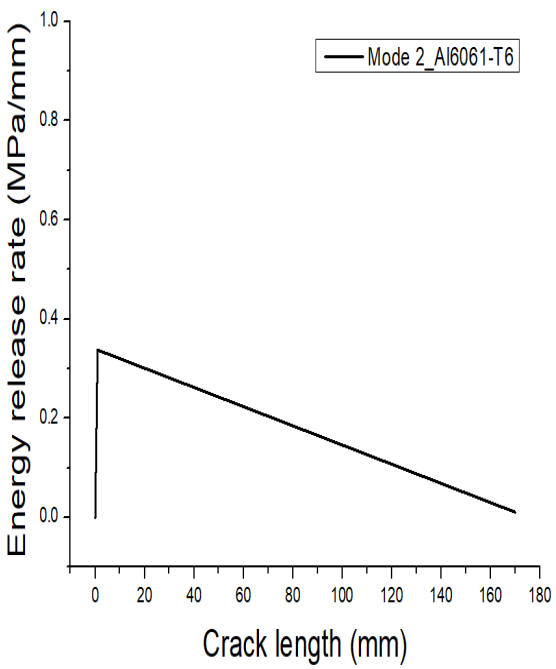

Fig. 12 Energy release rate due to crack length for the sliding fracture of mode II by Al6061-T6

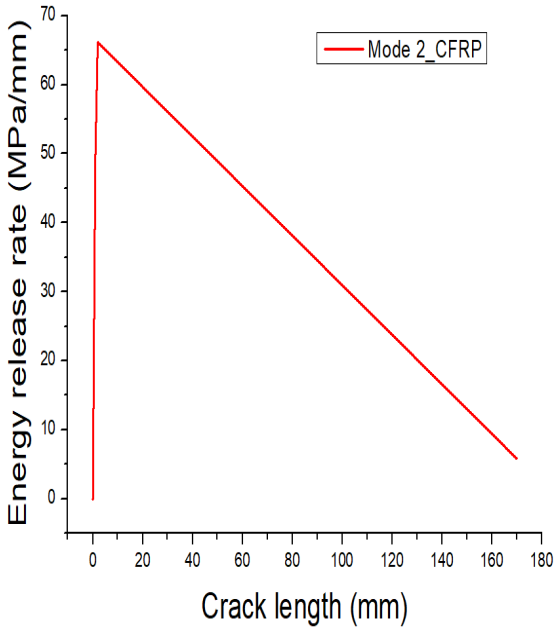

Fig. 13 Energy release rate due to crack length for the sliding fracture of mode II by CFRP

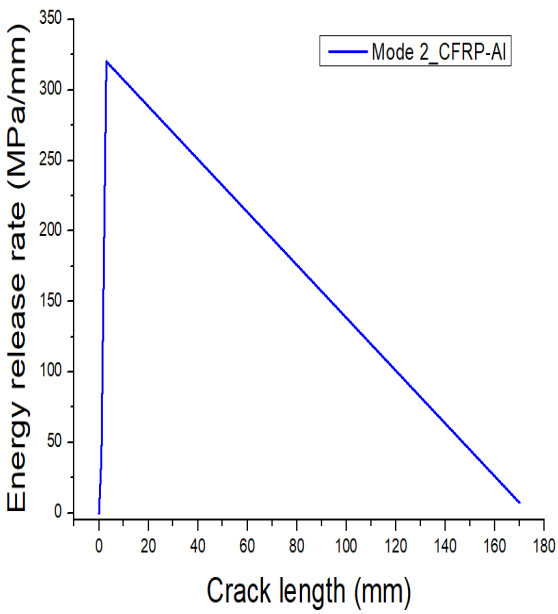

Fig. 14 Energy release rate due to crack length for the sliding fracture of mode II by CFRP-Al

In terms of the maximum energy release rate, ‘CFRP-Al’ was the highest, followed by CFRP and Al. The maximum energy release rates of ‘CFRP-Al’, CFRP and Al were 320 MPa/mm, 67 MPa/mm and 3 MPa/mm, respectively. By comparing with each other, the inhomogeneous material of ‘CFRP-Al’ was highest at the maximum energy release rate during the sliding fracture. Unlike the opening fracture, CFRP was higher than Al in terms of the stress and energy release rate.

5. Conclusion

This study was conducted on the fracture characteristic of bonded interface as a sliding load was applied to the double cantilevered specimen manufactured with the lightweight material. the results are concluded as follows;

1. In order to investigate the strength of the bonded interface of each material, the graphs of stress according to the displacement were investigated. Also, the maximum stress and the time point at which the maximum stress happened were examined. It was found that the stress was high in the order of CFRP-Al, CFRP, and Al. Also, in case of the material with the high strength, the time point at which the maximum stress happened appeared later.
2. All of the materials used in the study were the materials with good strength as compared to weight. And the specific strengths due to the materials were compared. It was seen that the specific strength was high in the order of CFRP, CFRP-Al, and Al. The lower the specific gravity, the higher the specific strength.
3. The energy release rate according to the crack propagation were compared with each other. It was found that the maximum energy release rate was high in the order of CFRP-Al, CFRP, and Al. In the very instant when the maximum energy release rate happened, it could be seen that the same initial crack appeared at all materials.
4. With these experimental results, it was found that CFRP was excellent in terms of the specific strength. Also, it was possible to prove that the inhomogeneous bonded material composed of CFRP-Al showed the high performance overall in comparison with the single materials.

Acknowledgements

This research was supported by the Basic Science Research Program through the National Research Foundation of Korea(NRF) and funded by the Ministry of Education(NRF-2018R1D1A1B07041627).

References

1. Ryu, C. W. and Choi, S. D., "Characteristics of Surface Roughness According to Wire Vibration and Wire-cut Electric Discharge Machining of Aluminum Alloy 6061 (Ⅲ)," Journal of the Korean Society of Manufacturing Process Engineers, Vol. 15, No. 1, pp. 81-88, 2016.
2. Park, J. W. and Cho, J. U., “Analysis Study of MT(Middle Tension) Specimen Laminated for Sandwich Structure with Aluminum-6061 and Aluminum Foam,” Journal of the Korean Society of Mechanical Technology, Vol. 20, No. 2, pp. 220-225, 2018.
3. Jung, M. W., Kwak, T. S., Kim, M. K. and Kim, G. H., "Effects of Ultrasonic Vibration on Machined Surface of Aluminium 6061 in Endmill Cutting Process," Journal of the Korean Society of Manufacturing Process Engineers, Vol. 13, No. 3, pp. 96-102, 2014.
4. Won, S. J., Li, C. P., Park, K. M. and Ko, T. J., "The Exit Hole Burr Generation of CFRP with Ultrasonic Vibration," Journal of the Korean

Society of Manufacturing Process Engineers, Vol. 16, No. 1, pp. 134-140, 2017.
5. Lee, J. H., Kim, E. D. and Cho, J. U., “Convergence Study on Damage and Static Fracture Characteristic of the Bonded CFRP structure with Laminate angle,” Journal of the Korea Convergence Society, Vol. 10, No. 1, pp. 155-161, 2019.
6. Han, M. S., Choi, H. K., Cho, J. U. and Cho. C. D., “Fracture property of double cantilever beam of aluminum foam bonded with spray adhesive,” Journal of Mechanical Science and Technology, Vol. 291, No. 1, pp. 5-10, 2015.
7. Kim, J. W. and Cho, J. U., “A Study on The Fracture Characteristics of Notch Hole Generation at Inhomogeneous Material Bonded with CFRP and Al-Foam Materials Using Finite Element Method,” Journal of the Korean Society of Mechanical Technology, Vol. 21, No. 4, pp. 574-579, 2019.
8. Lee, J. H., Choi, H. K., Kim, S. S., Cho, J. U., Zhao, G., Cho, C. and Hui, D. “A study on fatigue fracture at double and tapered cantilever beam specimens bonded with aluminum foams,” Composites Part B, Vol. 103, No. 15, pp. 139-145, 2016.
9. Kim, J. W., Jung, C. H. and Cho J. U., “A study on fracture characteristic of structural adhesive at bonded specimen made by 3D printer,” Journal of Mechanical Science and Technology, Vol. 34, No. 8, pp. 3295-3302, 2020.
10. Kim, J. W., Cho, C. D. and Cho, J. U., “A study on adhesive characteristics of double cantilever beam specimens with inhomogeneous materials due to tensile and out-of-plane shear fractures,” Composites Part B, Vol. 185, No. 15, pp. 1-7, 2020.
11. Kim, J. W. and Cho, J. U., “Fracture properties on the adhesive interface of double cantilever beam specimens bonded with lightweight dissimilar materials at opening and sliding modes,” Composites Part B, Vol. 198, No. 1, pp. 1-7, 2020.